

EXPERIMENTAL VALIDATION OF A DUAL LOOP CONTROL OF TWO PHASES INTERLEAVED BOOST CONVERTER FOR FUEL CELL APPLICATIONS

O. Kraa^{1,*}, H. Ghodbane¹, R. Saadi¹, M.Y. Ayad², M. Becherif³, M. Bahri¹ and A. Aboubou¹

¹Department of Electrical Engineering MSE Laboratory, Mohamed khider University Biskra, Algeria

²Industrial Hybrid Vehicle Applications, France

³FCLab FR CNRS 3539, Femto-ST UMR CNRS 6174, UTBM, France

Received: 27 December 2015 / Accepted: 15 April 2016 / Published online: 01 May 2016

ABSTRACT

In this paper, a modelling, an implementation and a control of a dc-dc converter structure called “two phases Interleaved Boost Converter (IBC)” will be presented. This topology is widely used in order to reduce the input current ripples and the size of passive component with high efficiency. The control of the IBC converter is designed by dual loop control that contains a voltage loop with a linear PI controller and a fast current loop with a non-linear sliding controller to ensure a good tracking in steady state and fast performance in transient state. The proposed control loop has been validated, first by the simulation results under Matlab-Simulink and after by the experimental results using a small-scale test bench with the dSPACE-1104 card.

Keywords: Interleaved Boost Converter; fuel cell; PI; sliding mode control.

Author Correspondence, e-mail: o.kraa@mse-lab.org

doi: <http://dx.doi.org/10.4314/jfas.v8i2.11>

1. INTRODUCTION

The depletion of fossil fuels and the global concern over the harmful emissions by their combustion has been a major cause of development of alternative approaches to meet new



energy requirements [1-3]. Fuel Cells (FCs) are an energy conversion devices that produce electrical energy from an electrochemical reaction between hydrogen-rich fuel gas and oxidant (air or oxygen). The main by-products are water, carbon dioxide, and heat. FCs are similar to batteries since they both produce a DC voltage by using an electrochemical process [4]. Unlike batteries, FCs does not release storage of energy; instead they convert energy from hydrogen-rich fuel directly into electricity.

Among the various FC existing technologies, the Proton Exchange Membrane Fuel Cell (PEMFC) is considered as the suitable technology for distributed generation and transport applications [5], thanks to its produce water as a residue, high efficiencies for powering vehicles, solid electrolyte and favorable power-to-weight ratio offer an order of magnitude higher power density than any other fuel cell type. It has also low corrosion, low temperature operation and it needs less time for starting and reaching its nominal operation conditions [6]. All these characteristics are needed for electrical vehicle applications.

However, some constraints are still of concern, especially its slow dynamic and low output voltage characteristic. To go over these two particular constraints, several cells should be stacked to attain the required output voltage that is often fixed close to 100 V and a DC/DC converter is then added to boost the output voltage of the FC to a high voltage DC bus. Such DC/DC converter is required not only for the voltage boost, but also for the voltage conditioning as the FC output voltage varies strongly with the load and for reducing the current ripple [7]. These DC/DC converters must respond to challenging issues in transportation applications such as [8]:

- High efficiency;
- Decrease the input ripple current for prolonging fuel cell lifetime;
- Weight and volume reduced;
- High power density;
- Low cost.

The interleaved boost converter (IBC) [9] is considered a good solution for improving the FC performances in steady and transient states, with respecting to the efficiency and current distribution. The concept of interleaving allows reducing the input current ripple which is one of the most important required characteristics from DC/DC converters for FC electric vehicle

(FCEV) and provides a high power, modularity and improved reliability. This work presents the control of two phases IBC coupled PEMFC with a load, the control of the converter is assured by dual loop initially contains a linear PI voltage loop controller and a fast current loop with a nonlinear sliding controller. Simulation and experimental results using a small-scale test bench with the dSPACE-1104 card results will be presented to validate the efficiency of the proposed control method.

The first subtitle opens with an introduction that presents the specific problem under study and describes the research strategy. The first subtitle opens with an introduction that presents the specific problem under study and describes the research strategy. The first subtitle opens with an introduction that presents the specific problem under study and describes the research strategy. The first subtitle opens with an introduction that presents the specific problem under study and describes the research strategy [1].

2. WHY TWO PHASES INTERLEAVED BOOST CONVERTER

The interleaved boost dc-dc converter is proposed to deal with the high current problems at high power applications. The Fig. 1 shows the schematic diagram of the interleaved boost dc-dc converter, consisting of a two identical elementary boost converters connected in parallel and sharing a common DC bus. The two identical parallel cells provide half of the total power each, where elementary Boost is controlled via the same duty cycle D and control signals are shifted by a half period. It's important to note that for a given duty cycle, this structure gives an output voltage same as in classical Boost structure and its major use advantage is [10]:

- 1) Increasing the overall converter efficiency;
- 2) Increase the input and output ripple frequency without increase the switching frequency;
- 3) Decrease the input ripple current;
- 4) Enhance the system reliability by paralleling phases.

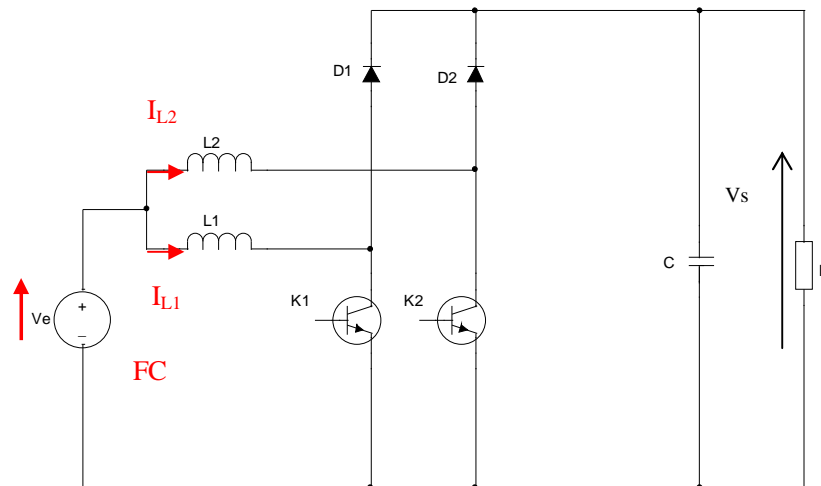


Fig.1. Interleaved 2-phases boost DC/DC converter

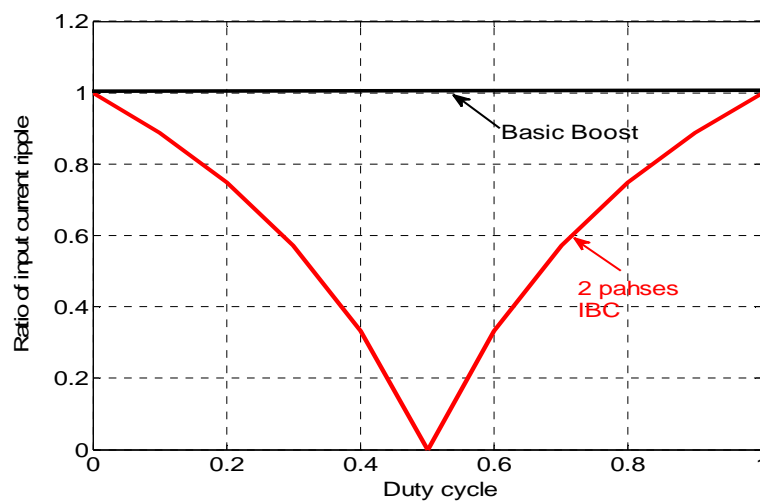


Fig.2. Ratio of input current ripple to phase inductor current ripple according to duty cycle

Another reason for this choice of topology is the cancellation of the ripple current for specific duty cycles. For the two phases IBC converter, the input current ripple equals zero for one specific value of duty cycle equals 0.5. The Fig. 2 shows the variation of the ratio of FC current ripple, Δi_{fc} to phase inductor current ripple, Δi_{Lx} according to the duty cycle for basic boost topology used usually for FC applications [11] and IBC two phases converter.

3. MODELING OF THE FC AND IBC SYSTEM

The studied system here is considered as a power train system for electric vehicle application (Fuel cell vehicle). It constituted by a FC (energy source) connected with a load through an IBC converters in order to ensure a high voltage ratio and a small power source current

undulation as shown in Fig. 1.

3.1. Fuel cell modeling

The output voltage of a single cell VFC can be defined as the result of the following equation [12]:

$$V_{FC} = E_0 - A \log \left(\frac{i_{FC} - i_n}{i_0} \right) - \left\{ R_m (i_{FC} - i_n) + B \log \left(1 - \frac{i_{FC} - i_n}{i_{Lim}} \right) \right\} \quad (1)$$

where E is the thermodynamic potential of the cell representing its reversible voltage, i_{FC} is the delivered current, i_0 is the exchange current, A is the slope of the Tafel line, i_{Lim} is the limiting current, B is the constant in the mass transfer, i_n is the internal current and R_m is the membrane and contact resistances. Hence $V_{FC} = f(i_{FC})$.

The second term of the voltage FC equation is the voltage drop due to the activation of the anode and of the cathode. The third term is the ohmic voltage drop, a measure of the ohmic voltage drop associated with the conduction of the protons through the solid electrolyte and electrons through the internal electronic resistances. The fourth term represents the voltage drop resulting from the concentration or mass transportation of the reacting gases.

This static model of FC is compared with the experimental results using PEMFC Nexa Ballard 1.2KW (Fig. 4). As it can be observed that the static model presented in (1) allows giving an excellent fit with the experimental results of polarization curve.

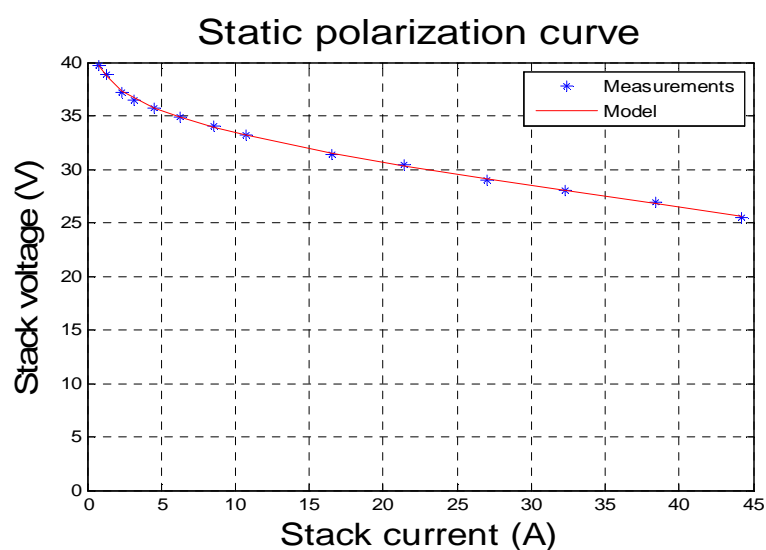


Fig.3. Experimental polarization curve and model

3.2. Two phases IBC modeling

To design the appropriate controller with required performances, it's important to do not neglect the dynamic considerations. Thus, A number of ac equivalent circuit modeling techniques have been presented in the literature, such as state-space-averaged modeling and PWM switch method for modeling DC-DC converters [13]. Among these methods, the PWM switch method is the widely used one to model DC-DC converters. The transfer functions for duty-cycle to inductor current $G_{ix}(s)$ and inductor current to the output voltage $G_{vx}(s)$ of IBC topology are obtained from averaged small-signal model are [ref]:

$$G_{ix}(s) = \frac{\tilde{i}_{Lx}}{\tilde{d}} = \frac{2V_1}{R(1-D)^2} \frac{1 + \frac{RC}{2}s}{1 + \left(\frac{L}{R(1-D)^2}\right)s + \left(\frac{LC}{(1-D)^2}\right)s^2} \quad (2)$$

$$G_{vx}(s) = \frac{\tilde{v}_s}{\tilde{i}_{Lx}} = \frac{R(1-D)}{2} \frac{1 - \left(\frac{L}{R(1-D)^2}\right)s}{1 + \left(\frac{RC}{2}\right)s} \quad (3)$$

Where \tilde{i}_{Lx} , \tilde{d} , \tilde{v}_s are small increments around of their operating points.

4. PROPOSED CONTROL STRATEGY OF THE TWO PHASES IBC CONVERTER

The correct design of the controller is a difficult task because according to equations (2) and (3), the transfer functions of IBC converter are of the 1st and 2nd order and its parameters vary strongly with the load changes. Then, it is essential to establish the control objectives, which can be formulated as following:

- Maintain the output voltage constant under load change;
- Equal current sharing between phases. The input current waveforms must be equal in order to avoid overloading one of the phases, particularly for heavy loads. Furthermore, the phase currents must be correctly shifted from each other in order to minimize the input current ripple which is undesirable in fuel cell applications;
- Ensure always the stability and dynamic performances of the closed-loop system with an acceptable overshoot and steady error.

4.1. Dual Loop Control

In this work, we proposed to control the two phases IBC by using a dual loop control that contains a linear PI outer loop (or voltage loop), which allows usefully comparing the output voltage reference with the measured output voltage of the two phases IBC converter. Hence, the total current reference is obtained from PI controller and then is shared out between each IBC phases. For the IBC topologies, the total current is divided on 2 (number of phase). Then, the inner loop (or current loop) allows us obtaining the duty cycles (D1, D2,) from nonlinear sliding mode controllers as it is shown in Fig. 4.

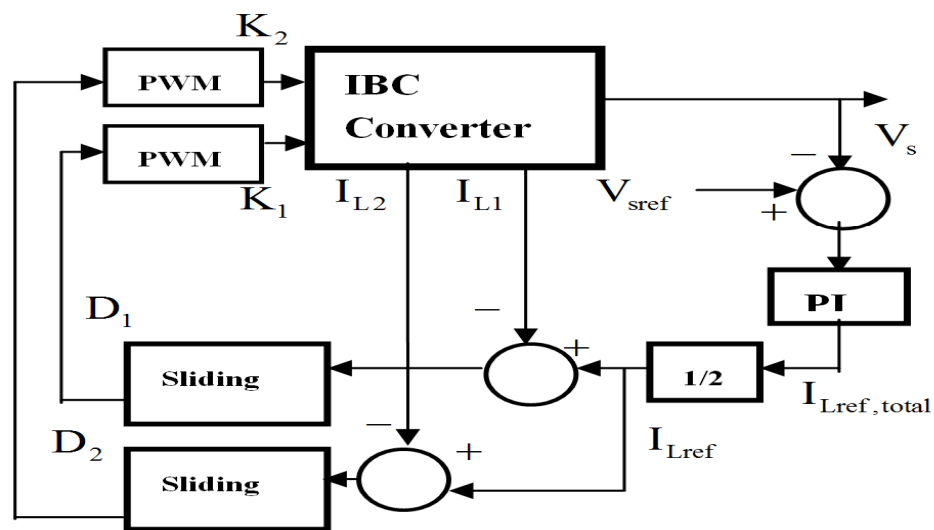


Fig.4. Control strategy architecture

The PI controller (PI-1) is defined as follow:

$$PI_1 = K_1 \left(1 + \frac{1}{T_1 s} \right) \tag{4}$$

The PI controller has been designed in order to satisfy the control objectives and some design requirements such as phase margin (PM), gain margin (GM) and settling time. In summary, they lead to the satisfactory performance, namely PM=45° and GM=10dB.

4.2. Current sliding mode controller

To ensure the stability and the robustness of the system, one has to control the inductive current. A nonlinear sliding mode controller is used to drive the current control loop applying the large signal model of DC-DC converters [14-16]. Thus, its stability is not restricted to be

around the operating point (as it is often in small signal modeling). The following equation defines the large signal model of the two phases IBC:

$$\begin{cases} L_1 \cdot \frac{dI_{L_1}}{dt} = V_e - (1 - D_1) \cdot V_s - r_{L_1} \cdot I_{L_1} \\ L_2 \cdot \frac{dI_{L_2}}{dt} = V_e - (1 - D_2) \cdot V_s - r_{L_2} \cdot I_{L_2} \\ C \cdot \frac{dV_s}{dt} = -I_{ch} + (1 - D_1) \cdot I_{L_1} + (1 - D_2) \cdot I_{L_2} \end{cases} \quad (5)$$

Where D_1 and D_2 correspond to the duty cycles for controlling the switches K_1 and K_2 respectively.

The sliding surfaces, then the control laws, of the IBC are defined by the following expression:

$$S_{iL_i} = (I_{L_i} - I_{L_{i,ref}}) + k_{iL} \int_0^t (I_{L_i} - I_{L_{i,ref}}) dt \quad (6)$$

Where $i = [1, 2]$, I_{L_i} is the average value of the inductors currents, $I_{L_{i,ref}}$ is the desired inductors currents, k_{iL} is the damping coefficients, which ensure that the sliding surface equal zero by tracking the inductor current to its reference is defined as follows:

$$\dot{S}_{iL_i} = -\lambda_{iL} S_{iL_i} \quad (7)$$

Where λ_{iL} is the convergence factor.

To design the controller, it is necessary to combine (5) with (6) and (7) for the two phases IBC. This will result in the equation for control inputs in terms of the state variables and the system parameters. The duty cycle of each phase of the IBC is:

$$D_i = 1 - \frac{V_e - r_{L_i} \cdot I_{L_i} + L_i \left(\lambda_{iL} S_{iL_i} - \dot{I}_{L_{i,ref}} + K_{iL} \cdot (I_{L_i} - I_{L_{i,ref}}) \right)}{V_s} \quad (8)$$

Equation (8) shows that the control inputs are irrelevant with the value of load resistance R . Therefore, this controller will not be perturbed by the variations of the load.

By injecting the values of duty cycles in the average model one can define the dynamic behaviour of the current error as follows:

$$\dot{z}_i + (\lambda_{iL} + k_{iL}) \cdot z_i + \lambda_{iL} \cdot k_{iL} \cdot \int z_i \cdot d\tau = 0 \quad (9)$$

Where $z_i = I_{Li} - I_{Lref}$.

After derivation the previous equation is given by

$$\ddot{z}_i + (\lambda_{iL} + k_{iL}) \cdot \dot{z}_i + \lambda_{iL} \cdot k_{iL} \cdot z_i = 0 \quad (10)$$

These equations are used to define the coefficients K_{iL} and the convergence factors λ_{iL} to ensure the desired performance. The coefficients are positive. So this signifies that all of system roots have strictly a negative real part. This involved the stability of the regulator.

5. SIMULATION RESULT

The whole FC pack and the used converter had been simulated under the Matlab-Simulink Software, the Table. 1 shows the system parameters.

Table 1. System parameters

Parameters	Value
Input voltage	42V
Output voltage	150V
Inductor value	1mH
Capacitor value	1100uF
ESR of the inductor	0.8 mΩ
Load resistor	6Ω
Switching frequency	10 KHZ

To test the two sliding mode current regulators of the two phases of IBC, the reference current is varied for observing the current behaviors of each phase .

The Fig.6 and 7 represent the evolution of the inductor current after the variation of the reference inductor current from 20 to 10A, from 20 to 40A and inversely, respectively. One can see that the currents track perfectly their references with a fast settling time (around 10^{-3})

with no noticeable ringing or overshoot (First order system behaviour). So the sliding mode current regulator gives excellent performances in transient and steady states of system.

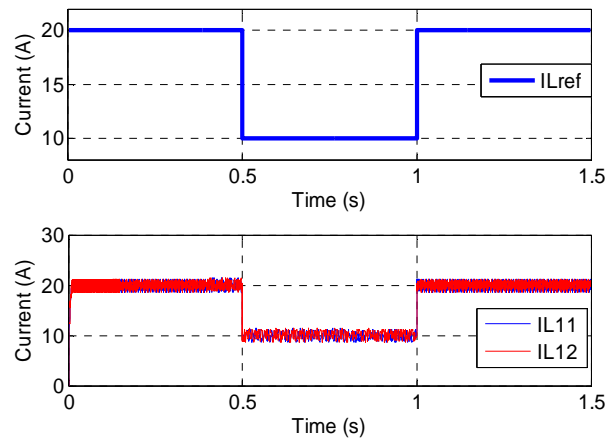


Fig.5. Sliding-mode controller dynamic response while the variation of inductor current from 20 to 10 A

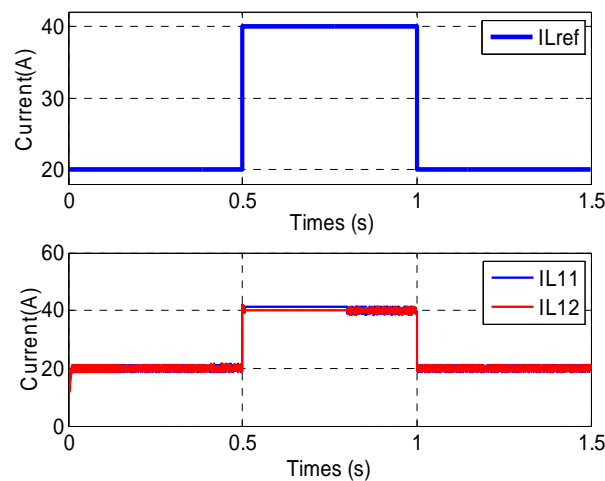


Fig.6. Sliding-mode controller dynamic response while the variation of inductor current from 20 to 40 A

Figures 8 to10 show the system responses under the dual loop control for the load stepping up of the rated conditions. By analysing those figures, it is possible to observe that the output voltage overshoot and oscillations are negligible, and the currents of inductors, which controlled by the sliding mode regulators respond very quickly and follow their reference perfectly and without any overshoot and oscillations. Figures11 to 13 represent the responses of the system while the load stepping down of the rated conditions. From this curves, one can

deduce that the output voltage set to its reference perfectly and the inductor currents follow well their references.

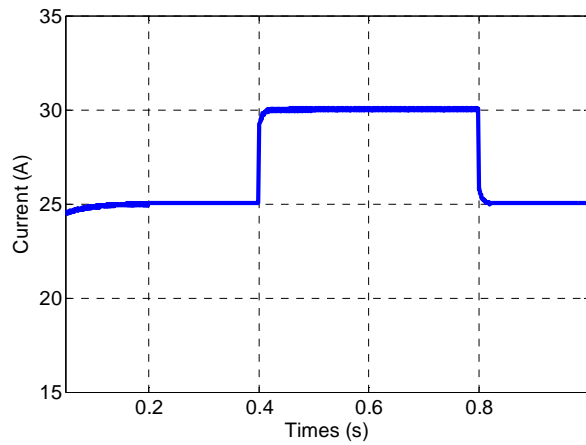


Fig.7. Load increasing and then coming back to rated load

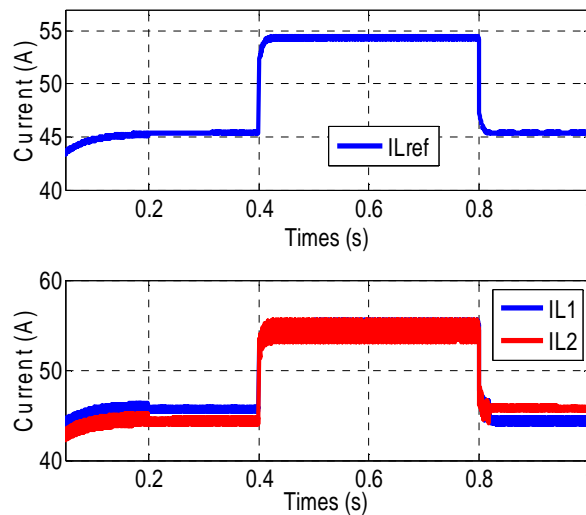


Fig.8. Inductor currents and their reference

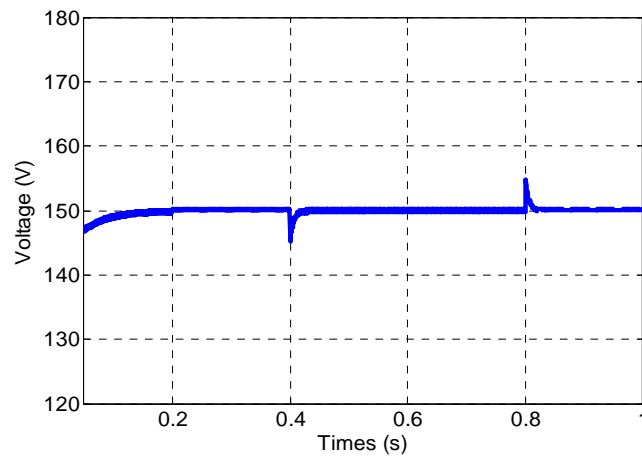


Fig.9. Output voltage response

Fig.14 shows the behaviour of the output voltage after changing the reference of output voltage from 150 to 110V and from 140V and inversely, respectively. Finally, the simulation results prove that the proposed dual loop control contains voltage loop with PI regulation and non-linear sliding mode current regulator has high dynamic performances in transient state (fast and without a considerable overshoot) even during the load stepping up or down, also while a reference changing.

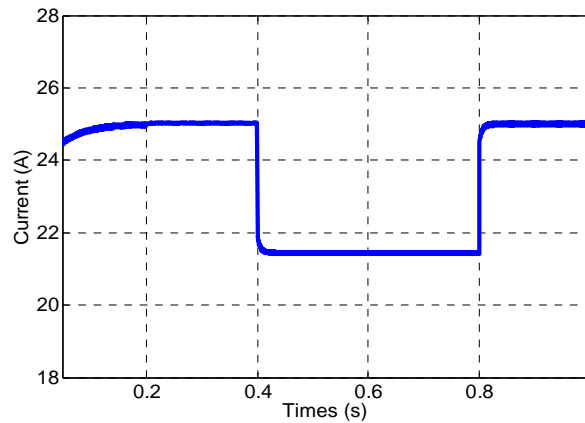


Fig.10. Load current profile

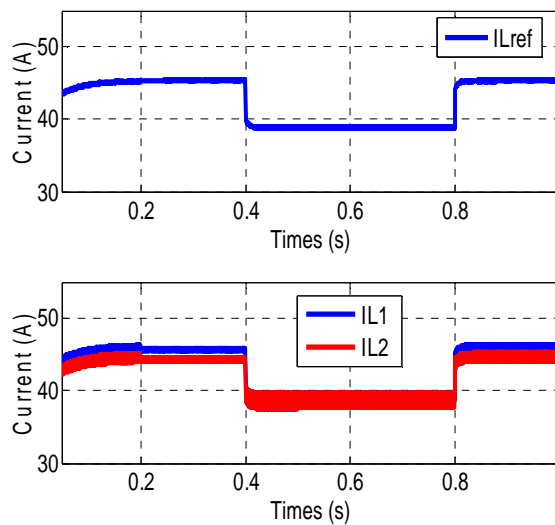


Fig.11. Inductor currents while the load change

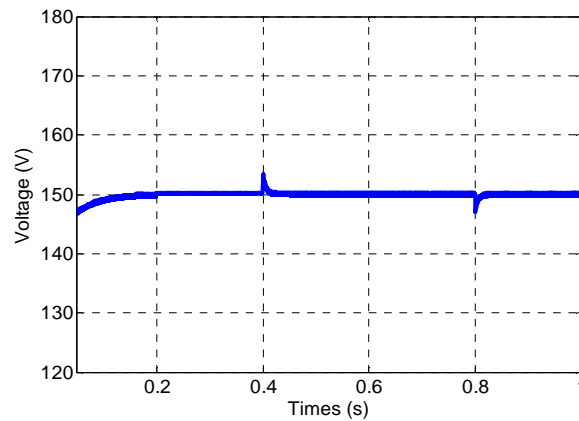


Fig.12. Output voltage while the load changing

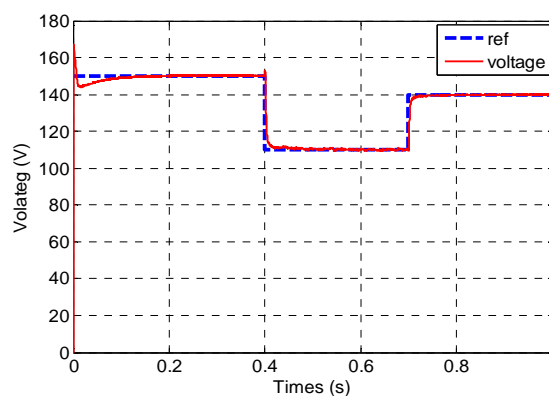


Fig.13. Output voltage and its reference

6. EXPERIMENTAL RESULTS

In order to validate the proposed control strategies of the two phases IBC structure connected with a FC, a small-scale test bench (150W) of the system is implemented in our laboratory. Fig. 14 shows the photograph of the realized experimental testbench of converter at Energy System Modelling Laboratory (ESM) in Biskra, Algeria. In this testbench, we replaced the FC by a programmable DC source to supply a resistive load through the IBC. The control is realized under the Matlab-Simulink-RTW software and implemented owing to the DSPACE-1104 real-time control card. As the converter connected to the load is controlled such that the the DC bus voltage (V_s) is 100V. The experimental validation has been done by using the following system parameters given in Table II.

Table 2. System parameters

Parameters	Value
Input voltage	25V
Output voltage	100V
Inductor value	10mH
Capacitor value	2200uF
ESR of the inductor	0.8 m Ω
Load resistor	75 Ω
Switching frequency	10 KHZ

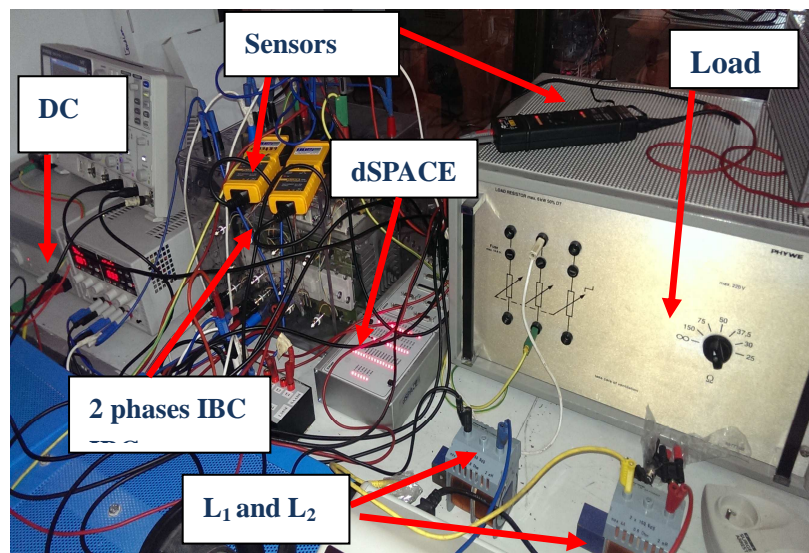


Fig.14. The realized test bench at ESM Laboratory

The Figs. 15 and 16 present the behaviour of inductor currents (I_{L1} and I_{L2}), while their reference profile changing, whereas, the Figs. 18 and 20 present their behaviour while the test is performed by sharply decreasing and increasing the load current I_{ch} (Fig. 17 load stepping up to 100 %, Fig. 20 load stepping down to 60 % of the rated condition). It is clear that the IBC currents track well their reference with an acceptable overshoot, a short response time and a stable steady state. Furthermore, the good tracking of the inductor currents to their references shows that the used sliding mode regulators work favourably.

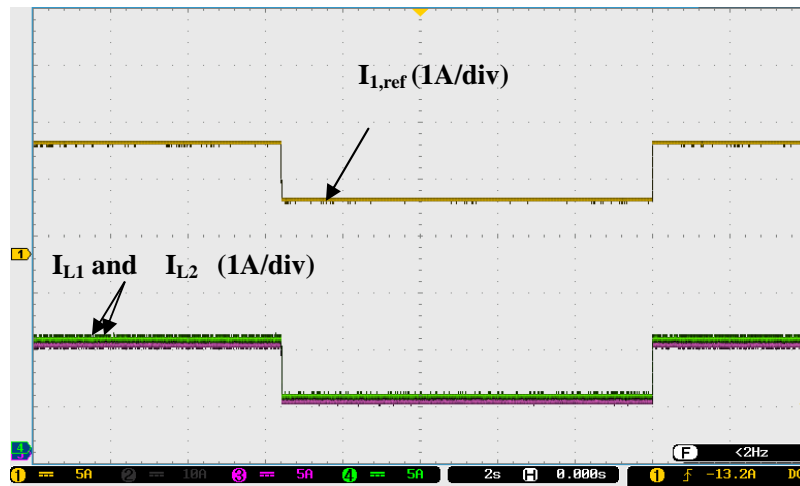


Fig.15. Inductor current responses and their reference variation (from 2 to 4 A)

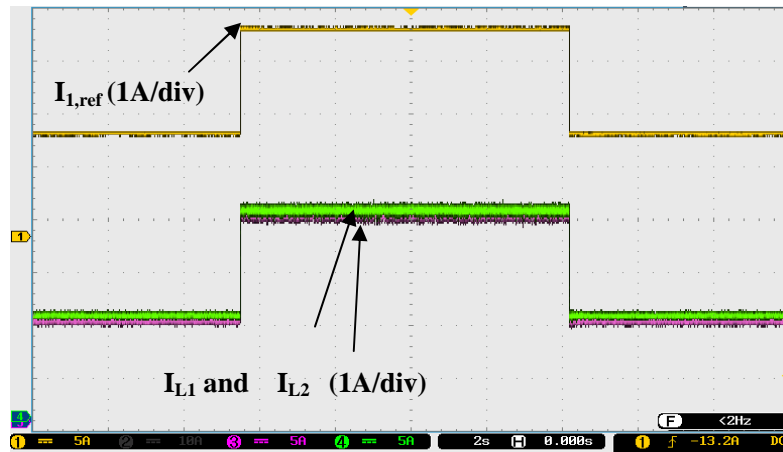


Fig.16. Inductor current responses and their reference variation (from 2 to 4 A)

The experimental results shown in Fig. 19 and 22 show that the controlled voltage V_s tracks well its even in presence of perturbation (load changings) from 100 to 120V and from 100 to 80V and inversely respectively.

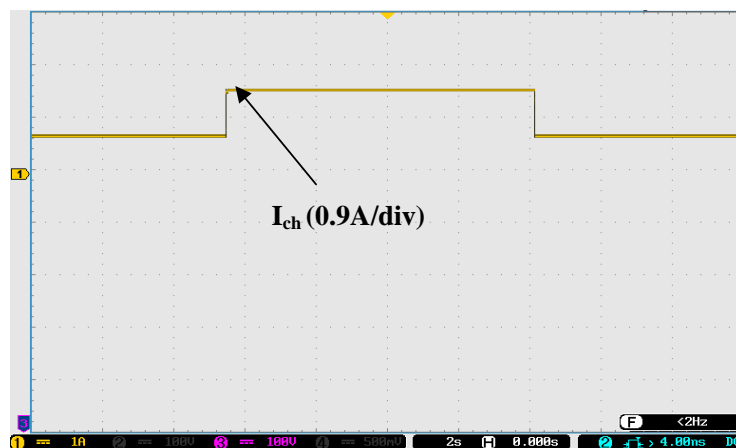


Fig.17. Load current profile (increasing with 100%)

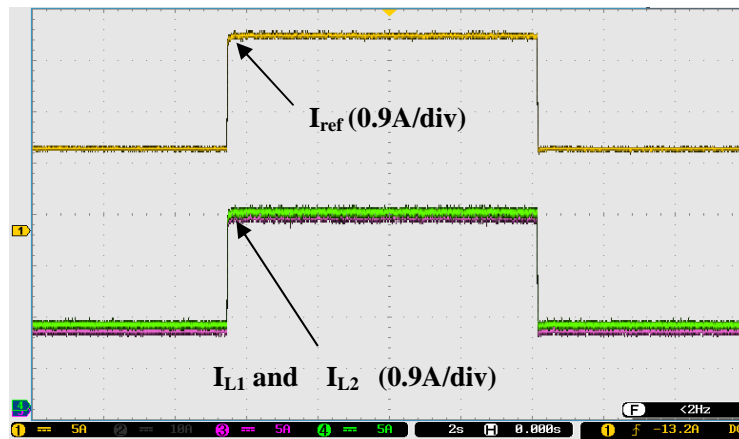


Fig.18. Inductor current responses and their reference variation while the increasing and decreasing of the load profile

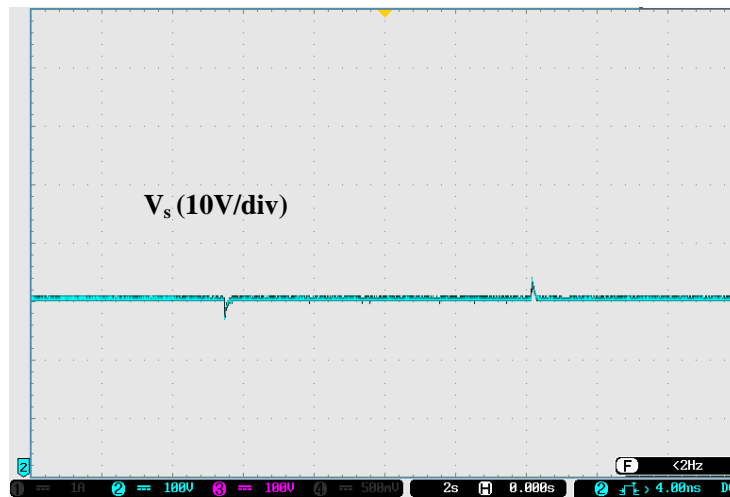


Fig.19. Output voltage after load increasing and then coming back to rated load

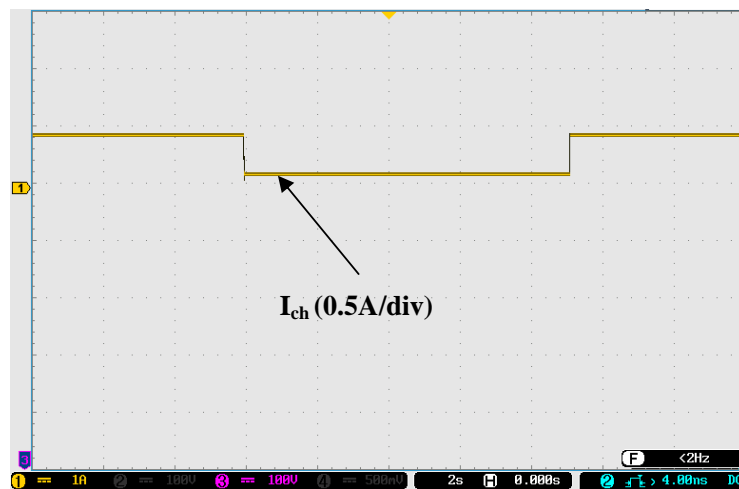


Fig.20. Load decreasing with 60% and then coming back to rated load

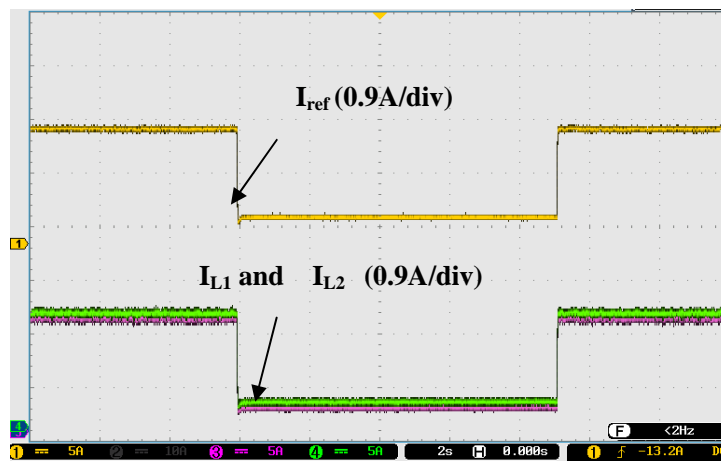


Fig.21. Inductor currents and their reference while the load decreasing and increasing

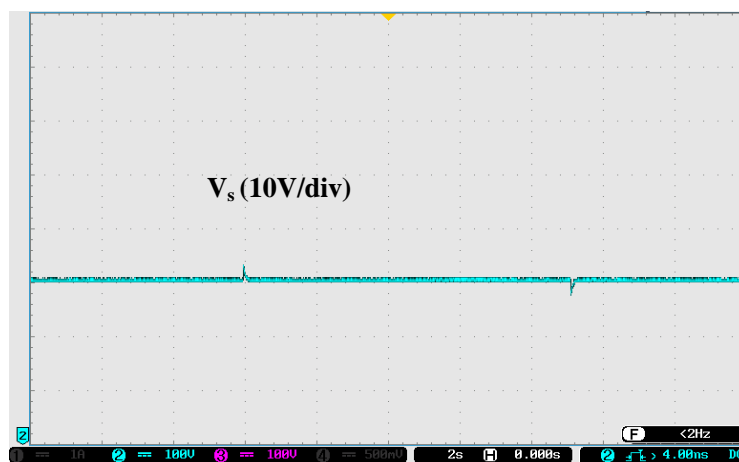


Fig.22. Output voltage the load decreasing and increasing

7. CONCLUSION

This paper presents an interleaved non-isolated DC/DC converter designed for fuel cell applications, simply for improving the performance because it ensures a high attenuation of the input current ripple, reduces the size of passive component and allows decrease semiconductor stresses, improving the converter efficiency and reliability. Whereas, the proposed dual-loop control strategy that contains a voltage loop with a linear PI controller and a fast current loop with a non-linear sliding controller is used and designed using PWM switch method in order to achieve a very good performance for a wide range of load variation and a stable and robustness behavior in presence of perturbations or parameter variations. Finally, the simulation and experimental results showed the good efficiency and functionality

of the converter and control strategy, which are suitable for FC applications, and especially in a power train system of an electric vehicle.

8. REFERENCES

- [1] Becherif M, Hissel D, Gaagat S, Wack M. Electrical equivalent model of a proton exchange membrane fuel cell with experimental validation. *Renewable Energy.*, 2011, 36, pp. 2582-2588.
- [2] Kishinevsky Y, Zelingher S. Coming clean with fuel cells. *IEEE Power and Energy Magazine.*, 2003, 1, pp. 20-25.
- [3] M. Becherif, M.Y. Ayad, D. Hissel and R. Mkahl, "Design and sizing of a stand-alone recharging point for battery electrical vehicles using photovoltaic energy", *Vehicle Power and Propulsion Conference, IEEE-VPPC'11*, 2011, pp. 1-6.
- [4] Ayad M, Becherif M, Henni A. Vehicle hybridization with fuel cell, supercapacitors and batteries by sliding mode control. *Renewable Energy*, 2011, 36, pp. 2627-2634.
- [5] M. Becherif, D. Hissel, S. Gaagat, M Wack, "Three order state space modeling of PEM Fuel Cell with energy function definition". *Journal of Power Sources*, 2010, 195 (19), pp. 6645- 6651.
- [6] Emadi A, Williamson S. Fuel cell vehicles: opportunities and challenges. in *IEEE Power Engineering Society General Meeting.*, 2004, pp. 1640-1645.
- [7] Kabalo M, Paire D, Blunier B, Bouquain D, Simões M G, Miraoui A. Experimental evaluation of four-phase floating interleaved boost converter design and control for fuel cell applications. *IET Power Electronics.*, 2013, 6, pp. 215-226.
- [8] Kabalo M, Paire D, Blunier B, Bouquain D, Simões M. G, Miraoui A. Experimental Validation of High-Voltage-Ratio Low-Input-Current-Ripple Converters for Hybrid Fuel Cell Supercapacitor Systems. *IEEE Transactions on Vehicular Technology.*, 2012, 61, pp. 3430-3440.
- [9] El Fadil H, Giri F, Guerrero J, Haloua M, Abouloifa A. Advanced Control of Interleaved Boost Converter for Fuel Cell Energy Generation System. in *World Congress.*, 2011, pp. 2803-2808.
- [10] Kabalo M, Blunier B, Bouquain D, Miraoui A. State-of-the-art of DC-DC converters for

fuel cell vehicles. in IEEE Vehicle Power and Propulsion Conference (VPPC)., 2010, pp. 1-6.

[11] Yu X, Starke M, Tolbert L, Ozpineci B. Fuel cell power conditioning for electric power applications: a summary. *IET Electric Power Applications.*, 2007, 1, pp. 643-656.

[12] Larminie J, Dicks A, and McDonald M S, Fuel cell systems explained. New York: Wiley, 2003, vol. 2.

[13] Kassakian J. G, Schlecht M. F, and Verghese G. C, Principles of power electronics, USA : Addison-Wesley Reading, 1991.

[14] El Fadil H, Giri F, and Guerrero J. M. Adaptive sliding mode control of interleaved parallel boost converter for fuel cell energy generation system. in *Simulation Mathematics and Computers.*, 2013, 91, pp. 193-210.

[15] Ayad M. Y, Becherif M, Djerdir A, Miraoui A. Sliding mode control for energy management of dc hybrid power sources using fuel cell, batteries and supercapacitors. In *International Conference on Clean Electrical Power ICCEP'07.*, 2007, pp. 500-505.

[16] Ayad M. Y, Becherif M, Miraoui A. Sliding Mode Control of DC Bus Voltage of a Hybrid Sources using Fuel Cell and Supercapacitors for Traction System. In *IEEE International Symposium on Industrial ElectronicsISIE 2007.*, 2007, pp. 383-388.

How to cite this article:

Kraa O, Ghodbane H, Saadi R, Ayad M.Y, Becherif M, Bahri M and Aboubou A. Experimental validation of a dual loop control of two phases interleaved boost converter for fuel cell applications . *J. Fundam. Appl. Sci.*, 2016, 8(2), 327-345.